

## Piezoelectric displacement sensing with a single-electron transistor

R. Knobel and A. N. Cleland<sup>a)</sup>

*Department of Physics and iQUEST, University of California at Santa Barbara, Santa Barbara, California 93106*

(Received 30 May 2002; accepted for publication 23 July 2002)

We propose a displacement sensing scheme for rf mechanical resonators made from GaAs, based on detecting the piezoelectrically induced charge. By using a single-electron transistor to detect the charge, we calculate that a significantly higher displacement sensitivity can be achieved than by using capacitive displacement sensing, primarily due to the strong piezoelectric coupling strength. We estimate a displacement sensitivity of order  $10^{-17}$  m/Hz<sup>1/2</sup> for a 1 GHz GaAs resonator. Our model solves the coupled electromechanical response self-consistently, including the effects of both dissipative and reactive electronic circuit elements on the resonator behavior. © 2002 American Institute of Physics. [DOI: 10.1063/1.1507616]

There is significant interest in developing detection schemes that might achieve quantum-limited displacement sensing of nanometer-scale resonators.<sup>1–3</sup> At present, one of the most promising approaches is to use a single-electron transistor (SET) capacitively coupled to a flexural beam resonator.<sup>1,4</sup> In this scheme, the flexural beam is biased with a constant voltage, so that its motion changes the charge coupled to a nearby SET, hence changing the current through the SET. Increasing the voltage applied to the beam leads to larger coupled charge signals, but also increases the back-action coupling between the SET and the beam. For a model cantilever and SET, applying the optimal bias voltage yields<sup>1</sup> a displacement sensitivity of  $4 \times 10^{-16}$  m/Hz<sup>1/2</sup>.

Here, we demonstrate that if instead the resonator is fabricated from a piezoelectric material, such as GaAs,<sup>3</sup> AlGaAs,<sup>5</sup> or AlN,<sup>6</sup> and the SET is configured to sense the piezoelectric voltage developed when the beam flexes, then a significantly higher displacement sensitivity can be achieved; we calculate a noise figure of  $5 \times 10^{-17}$  m/Hz<sup>1/2</sup>, dominated equally at peak sensitivity by the current and back action noise of the SET. This technique is similar to that of Beck *et al.*,<sup>7</sup> where an integrated field-effect transistor was used to sense strain. Here, the superior noise performance of the SET permits several orders of magnitude improvement in the displacement sensitivity.

In Fig. 1(a), we show the heterostructure design from which the device could be fabricated, and in Fig. 1(b), a schematic view of the doubly clamped resonator that includes the SET. The heterostructure includes a two-dimensional electron gas (2DEG) 50 nm below its surface, which acts as a ground plane for the actuation and detection signals. The device is fabricated using a sequence of electron-beam lithography, etching, and metal deposition to define the SET and the mechanical resonator.<sup>4</sup> The model resonator, with dimensions  $L \times w \times t = 0.64 \times 0.2 \times 0.1 \mu\text{m}^3$ , is designed to operate at the fundamental flexural frequency  $\omega_1/2\pi = 1.027(E/\rho)^{1/2}(t/L^2) = 1.0$  GHz, using Young's modulus  $E = 85$  GPa and  $\rho = 5.32$  g/cm<sup>3</sup> for GaAs.

Flexure of the resonator in the  $z$  direction, with the

$\langle 100 \rangle$  crystal axis aligned along  $z$ , will generate a piezoelectric polarization density  $\mathbf{P}$  along  $z$ , with the polarization amplitude proportional to the distance from the midpoint ( $z = 0$ ) of the beam.<sup>8</sup> The polarization induces a screening charge on the detection electrode, which can be detected by the SET. Conversely, when an electric field is applied between the actuation electrode and the 2DEG, along  $z$ , the beam will respond with an in-plane strain, which couples to the fundamental flexural mode. For a neutral axis displacement  $U(x)$ , the polarization density  $P(x, z)$  a height  $z$  above the neutral axis is  $P(x, z) = 0.315d_{14}EzU''(x)$ .<sup>9</sup> Here,  $d_{14} = 3.03$  pC/N is the relevant piezoelectric constant for Al<sub>0.3</sub>Ga<sub>0.7</sub>As.<sup>5,8</sup> For the fundamental flexural mode, the polarization density is largest at the beam surface  $z = t/2$ , and is maximum at the beam ends  $x = \pm L/2$ , crossing zero at  $x = \pm 0.276L$ , and reaching a secondary (negative) maximum at the beam center  $x = 0$ . This polarization induces a charge  $q$  on the detection electrode, which extends from the beam end to the zero-crossing point, over the full width  $w$  of the beam. The induced charge is the integral of the polarization at the surface,  $P(x, t/2)$ , over the area of the detection electrode.

The circuit connected to the detection electrode will affect the electromechanical response of the resonator (a somewhat related effect was described by Schwab).<sup>10</sup> The response can be determined by solving the coupled electrical

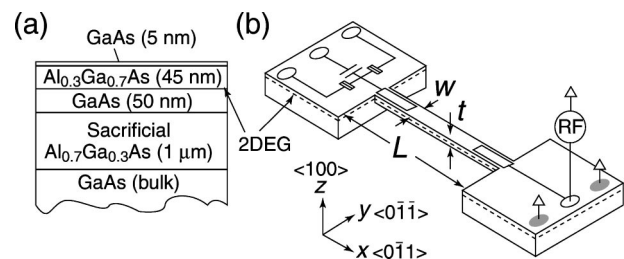


FIG. 1. (a) GaAs/AlGaAs heterostructure design; layer thicknesses indicated in parentheses. A 2DEG is formed at the GaAs-(modulation-doped) Al<sub>0.3</sub>Ga<sub>0.7</sub>As interface. Vertical axis is not to scale. (b) Sketch of device; the resonator has dimensions  $L \times w \times t$ , with the SET situated at one end of the beam, coupled to a detection electrode, with an actuation electrode that is driven by a rf source at the other end.  $V_g$  is the voltage applied to the gate of the SET, and  $V_{ds}$  the drain-source bias voltage. The GaAs crystal axes, and the geometric axes, are indicated.

<sup>a)</sup>Electronic mail: cleland@quest.ucsb.edu

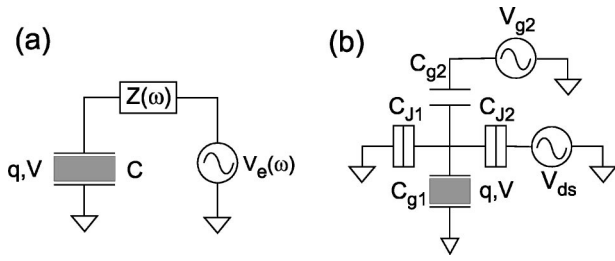


FIG. 2. (a) Nyquist equivalent circuit connected to the piezoelectric detection electrode, with impedance  $Z(\omega)$  and voltage source  $V_e(\omega)$ . (b) Circuit model for detection electrode as the island of the SET.

and mechanical equations of motion self-consistently. In a piezoelectric material, the stress, strain, electric field, and polarization density provide a complete description of the state of the system, and any pair of these can be chosen as the independent variables, the other two determined through the linear piezoelectric relations.<sup>11</sup> In our case, we consider only the fundamental flexural mode for the resonator, electrically coupled through the detection electrode shown in Fig. 1(b), and we simplify the full tensor relations to those involving the force  $F$  coupled to the fundamental mode shape, the displacement  $U=U(0)$  of the beam midpoint, and the charge  $q$  and voltage  $V$  induced on the detection electrode. These are then related to one another through the relations<sup>9</sup>

$$\begin{pmatrix} F \\ q \end{pmatrix} = \begin{pmatrix} k & a \\ a & C \end{pmatrix} \begin{pmatrix} U \\ V \end{pmatrix}. \quad (1)$$

Here,  $k=M\omega_1^2$  is the effective spring constant for a beam mass  $M$ ,  $C$  is the geometric capacitance associated with the detection electrode, and  $a$  is a scaled piezoelectric constant that relates the force to an applied voltage, for fixed displacement, and the induced charge to a displacement, for a fixed voltage. The material symmetries make the constants for these two relations equal. For the fundamental mode of our model GaAs/AlGaAs flexural resonator, we have  $k=2700$  N/m,  $C=0.448\epsilon\epsilon_0(wL/t)=65$  aF, and  $a=0.771d_{14}E(wt/L)=6.2\times 10^{-9}$  C/m.

The mechanical resonator response includes inertial and dissipative terms in the displacement  $U$ , and we model the electrical circuit as a Nyquist equivalent circuit with impedance  $Z(\omega)$  and voltage  $V_e(\omega)$ , as shown in Fig. 2(a). The coupled equations of motion, using Eq. (1), are then given by

$$\left. \begin{aligned} & \left( k - M\omega^2 + iM \frac{\omega\omega_1}{Q_m} + \frac{i\omega Z}{1+i\omega CZ} a^2 \right) U \\ & = F_D + \frac{1}{1+i\omega CZ} a V_e, \\ & q = \frac{aU + CV_e}{1+i\omega CZ} \end{aligned} \right\}. \quad (2)$$

For a real impedance  $Z(\omega)=R$ , at low frequencies  $\omega RC \ll 1$ , the circuit damps the resonator, giving a net quality factor  $1/Q_t = 1/Q_m + 1/Q_{el}$  with the electrical contribution  $Q_{el} = M\omega_1/a^2R$ . This type of damping has been observed with an atomic force microscope cantilever in carbon nanotube-based SETs.<sup>12</sup> If the force  $F_D$  is the thermomechanical noise at temperature  $T$ , with classical spectral density  $S_F(\omega) = 2k_B T M \omega_1 / \pi Q_m$ , and the resistor has Nyquist

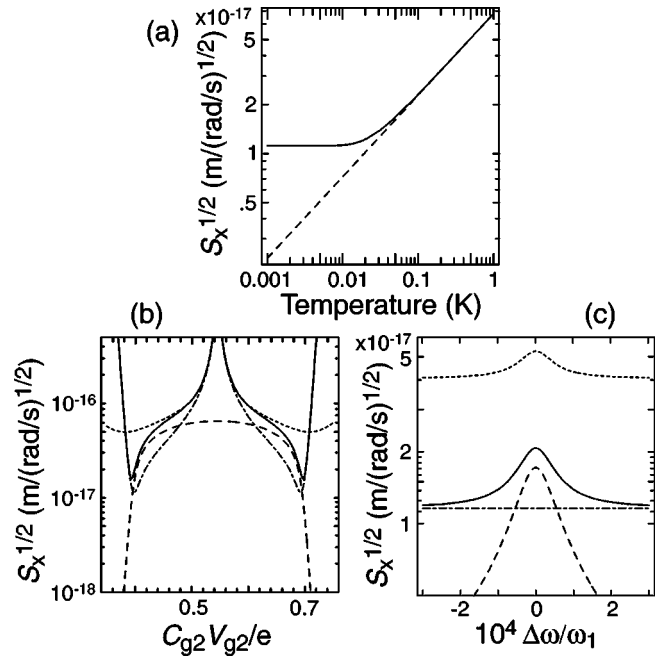


FIG. 3. (a) Displacement noise as a function of temperature, at the beam resonance frequency for the model beam. The dashed line is the classical thermal noise, while the solid line is the Callen–Welton noise. (b) Displacement noise as a function of gate voltage, at the beam resonance frequency for the model SET with  $V_{ds}=0.3e/C_\Sigma$  at 10 and 100 mK. (c) Displacement noise at  $V_{g2}=0.4e/C_{g2}$  as a function of frequency detuning from the beam resonance, showing the resonance response effect on the back-action noise. In plots (b) and (c), dashed lines are back-action noise  $S_X^B$ , dashed-dotted lines readout noise  $S_X^R$ , and solid lines total noise for 10 mK while dotted lines indicate the total noise for 100 mK.

voltage noise at temperature  $T$ ,  $S_V(\omega) = 2k_B T R / \pi$ , the effective force noise from Eq. (2) is that corresponding to thermomechanical force noise for a quality factor  $Q_t$ . The classical spectral density of the displacement noise  $S_X^T(\omega)$  at temperature  $T$ , including both the thermomechanical and electrical noise, is given by

$$S_X^T(\omega) = \frac{1}{(\omega_1^2 - \omega^2)^2 + (\omega\omega_1/Q_t)^2} \frac{2k_B T \omega_1}{\pi M Q_t}. \quad (3)$$

On resonance  $\omega = \omega_1$ , the displacement noise is  $S_X^T(\omega)^{1/2} = \sqrt{2k_B T Q_t / \pi M \omega_1^3}$ . For mechanical resonators at low temperatures, with  $\hbar\omega_1 \geq k_B T$ , we should use the Callen–Welton quantum formula for the noise,<sup>13</sup>  $S_F(\omega) = (\omega_1 / \pi M Q_t) \hbar \omega \coth(\hbar\omega / 2k_B T)$ , replacing the last ratio in Eq. (3). The temperature dependence of this displacement noise on resonance for the model beam with an assumed quality factor  $Q_t$  of  $10^4$  is plotted in Fig. 3(a). The quantum limited displacement noise of this beam is  $1.1 \times 10^{-17}$  m/(rad/s)<sup>1/2</sup>.

At high frequencies  $\omega RC \gg 1$ , the electrical circuit stiffens the mechanical response, shifting the resonance frequency without adding dissipation. In this limit, the voltage noise is reduced by the  $RC$  rolloff of the circuit.

For capacitive loading of the resonator, with  $Z = 1/i\omega C_e$ , the external circuit will only act to stiffen the effective mechanical response, so that the resonance frequency shifts to  $\omega_1'^2 = \omega_1^2 + a^2/MC_e$ .

We now analyze the displacement sensitivity of the piezoelectric resonator coupled to a SET, whose circuit is

shown in Fig. 2(b). In order to measure the motion of the beam at the resonant frequency, the SET can either be used with a resonant tank circuit<sup>14</sup> (termed rf-SET), or can be used as a rf mixer;<sup>4</sup> in the latter implementation, operation at frequencies up to and above 1 GHz is achievable. These frequency-shifting techniques should not significantly modify the noise analysis presented here.

The displacement sensitivity is limited by two effects: The current noise of the SET  $S_I(\omega)$  adds to the detected displacement signal, generating a spectral noise density  $S_X^R(\omega)$  referenced to the beam displacement, which we term the readout noise. In addition, the fluctuation in the number of electrons on the SET center island causes the island voltage to fluctuate. This voltage noise actuates the beam resonator, providing a source of back-action noise, with displacement spectral density  $S_X^B(\omega)$  (again referred to the beam displacement). Semiclassical expressions for the noise of a SET have been developed by Korotkov;<sup>15</sup> here, we use the approximate model developed by Zhang and Blencowe,<sup>16</sup> which applies in the low-temperature limit  $k_B T \ll eV_{ds}$ , so that only terms involving  $n$  and  $n+1$  electrons on the SET island are kept.

With the resonator coupled to one input gate  $C_{g1}$  of the SET, the input impedance is that of the other island capacitances in parallel,  $Z(\omega) = 1/i\omega C'_\Sigma$  with total island capacitance  $C_\Sigma = C_{J1} + C_{J2} + C_{g1} + C_{g2} = C'_\Sigma + C_{g1}$ . The total displacement noise spectral density  $S_X(\omega)$ , referred to the beam displacement, is the sum of the contributions from the readout and back-action noise,

$$S_X(\omega) = S_X^R(\omega) + S_X^B(\omega), \quad (4)$$

where we ignore correlations between these two noise sources. The readout noise  $S_X^R(\omega)$  is related to the SET current noise  $S_I(\omega)$  by the displacement responsivity of the SET,

$$S_X^R(\omega) = S_I(\omega) / (dI_{ds}/dU)^2, \quad (5)$$

where  $dI_{ds}/dU$  is the derivative of the SET current with midpoint displacement  $U$ . From Eq. (2), we can relate the SET-coupled charge  $q(U)$  to the displacement  $U$  for fixed voltage  $V_e$ ,  $dq/dU = a/(1 + C_{g1}/C'_\Sigma)$ , and using the form for the SET current-charge dependence  $I_{ds}(q)$  we can determine the readout noise  $S_X^R$ . The back-action noise can be evaluated from the relation between displacement  $U$  and voltage  $V_e$  for fixed drive force  $F_D$ ; the voltage  $V_e$ , equal to the SET center island voltage, is related to the number  $n$  of electrons on the center island by  $V_e = (en + \tilde{q})/C_\Sigma$ , where  $\tilde{q}$  is the charge bias applied to the SET, assumed noiseless. From the expression<sup>16</sup> for the spectral density of the number

noise  $S_n(\omega)$ , we then have the spectral density of voltage noise  $S_V(\omega) = (e/C_\Sigma)^2 S_n(\omega)$ , and from Eq. (2), we can evaluate the corresponding back-action displacement noise  $S_X^B$ , with

$$S_X^B(\omega) = \frac{1}{(\omega_1'^2 - \omega^2)^2 + (\omega\omega_1/Q)^2} \left( \frac{aC'_\Sigma}{MC_\Sigma} \right)^2 S_V(\omega), \quad (6)$$

with the resonance frequency shifted by the circuit capacitance.

In Fig. 3, we display the two contributions as well as the total noise, calculated for an optimized SET with junction resistances  $R_{J1} = R_{J2} = 100$  k $\Omega$ , junction capacitances  $C_{J1} = C_{J2} = 0.15$  fF, and gate capacitances  $C_{g1} = C_{g2} = 65$  aF, at temperatures of 10 and 100 mK.

The detection of the piezoelectrically induced charge in a mechanical resonator with a SET has been shown to be a prime candidate for nearly quantum-limited displacement sensing. Piezoelectric detection is additionally attractive because the piezoelectric signals scale favorably to the small, stiff resonators needed to approach the regime where  $\hbar\omega_1 \geq k_B T$ . In both the capacitive and piezoelectric schemes, the detection of deviations from the classical motion will be difficult for nanomechanical resonators with  $\omega_1/2\pi < 1$  GHz.

The authors acknowledge the financial support provided by the National Science Foundation XYZ-On-A-Chip Program, Contract No. ECS-9980734, by the Army Research Office, and by the Research Corporation through a Research Innovation Award.

<sup>1</sup>M. P. Blencowe and M. N. Wybourne, Appl. Phys. Lett. **77**, 3845 (2000).

<sup>2</sup>A. D. Armour, M. P. Blencowe, and K. C. Schwab, Phys. Rev. Lett. **88**, 148301 (2002).

<sup>3</sup>A. N. Cleland, J. S. Aldridge, D. C. Driscoll, and A. C. Gossard, Appl. Phys. Lett. (to be published).

<sup>4</sup>R. Knobel, C. S. Yung, and A. N. Cleland, Appl. Phys. Lett. **81**, 532 (2002).

<sup>5</sup>S. Adachi, J. Appl. Phys. **58**, R1 (1985).

<sup>6</sup>A. N. Cleland, M. Pophristic, and I. Ferguson, Appl. Phys. Lett. **79**, 2070 (2001).

<sup>7</sup>R. G. Beck, M. A. Eriksson, M. A. Topinka, R. M. Westervelt, K. D. Maranowski, and A. C. Gossard, Appl. Phys. Lett. **73**, 1149 (1998).

<sup>8</sup>J. Söderkvist and K. Hjort, J. Micromech. Microeng. **4**, 28 (1994).

<sup>9</sup>A. N. Cleland and R. Knobel (unpublished).

<sup>10</sup>K. Schwab, Appl. Phys. Lett. **80**, 1276 (2002).

<sup>11</sup>B. Auld, *Acoustic Fields and Waves in Solids*, 2nd ed. (Wiley, New York, 1990).

<sup>12</sup>M. T. Woodside and P. L. McEuen, Science **296**, 1098 (2002).

<sup>13</sup>V. B. Braginsky and F. Y. Khalili, *Quantum Measurement* (Cambridge University Press, Cambridge, UK, 1992).

<sup>14</sup>R. J. Schoelkopf, P. Wahlgren, A. A. Kozhevnikov, P. Delsing, and D. E. Prober, Science **280**, 1238 (1998).

<sup>15</sup>A. N. Korotkov, Phys. Rev. B **49**, 10381 (1994).

<sup>16</sup>Y. Zhang and M. P. Blencowe, J. Appl. Phys. **91**, 4249 (2002).